

Study on the vibration characteristics of a phononic crystal split cylinder structure

Randy Amuaku^{1,2*}, Alexander Fordjour¹, Frank Agyen Dwomoh¹, Francis Otuboah¹, John Bonney¹, Kun Zhang², Yuanyuan Shi², Peter Konadu²

¹Koforidua Technical University, Faculty of Engineering, Koforidua, Ghana.

²School of Energy and Power, Jiangsu University of Science and Technology, Zhenjiang 212003, China

Abstract

The problem of low frequency vibration and noise is a huge challenge in most engineering systems and structures. Bandgap characteristics of a phononic crystal structure can be used to control the propagation of elastic and acoustic waves, providing a new direction for controlling low frequency vibration and noise. In this paper a periodic split cylinder with varying diameter and a soft material wave propagating scatterer inclusion is proposed. Finite element methods are used to analyze the vibration characteristics across the surface of a split cylinder structure using three impact excitation points along the z-direction of wave propagation. Using finite element calculation methods, a low frequency vibration bandgap was obtained between 48~70Hz and 83~128Hz. Experimental and numerical calculations show vibration characteristics in the low frequency range with a transmission loss of -165dB at an attenuation frequency of 270Hz.

Keywords: Phononic crystal (PCs), Phononic Bandgap characteristics (PBGs), Vibration characteristics, Low frequency, Finite element method (FEM), Perfectly matched layer (PML).

1. Introduction

Propagation of acoustic and elastic waves in periodic structures called phononic crystals (PCs) have attracted a lot of interest due to their extraordinary properties (Kushwaha, 1996; W. Xiao, Zeng, & Cheng, 2008). Composite structures exhibit rich physics such as negative refraction, localized defects modes and phononic band gaps (PBGs) (Cheng, Liu, & Wu, 2011; Ramakrishna, 2005). Through structural design, phononic crystals can have bandgap characteristics at certain frequency ranges, thus preventing the propagation of elastic waves. This new method of controlling elastic waves provides a new direction and thinking in the control of vibration and noise which has attracted much attention and research from many researchers (Del Vescovo & Giorgio, 2014; Maldovan, 2013; Sun, Jolly, & Norris, 1995). In particular, the local resonant phononic structure has excellent low frequency bandgap characteristics (Baravelli & Ruzzene, 2013; Hsu, 2011; Y. Xiao, Wen, & Wen, 2012). Its discovery and development not only mark another breakthrough in the study of phononic crystals (Sridhar, Kouznetsova, & Geers, 2016; Wagner et al., 2016), but also creates a situation for the application of phononic crystals in low frequency vibration and noise reduction (Jensen, 2003; Kushwaha, Halevi, Dobrzynski, & Djafari-Rouhani, 1993), (Lu, Feng, & Chen, 2009), researched into acoustic metamaterials, in their study they proposed the concept of local resonant phonon structure, which officially opened its introduction. Two basic types of mechanism are used in the generation of bandgaps which are the: Bragg scattering and local resonant (Goffaux & Sánchez-Dehesa, 2003; Laude, 2015; L. Liu & Hussein, 2012), both of which are the result of the interaction of the periodic structure and the Mie scattering of a single scatterer, but the former is mainly the periodicity of the structure (Kushwaha, 1996; Z. Liu, Chan, & Sheng, 2002; Shen, Wu, Liu, & Fu, 2015), and the wavelength of the incident elastic wave and the characteristic length of the structure (Aki & Larner, 1970; Su, Ye, & Lu, 2006). In a situation where the lattice constant is close, the incident waves will be strongly scattered by the influence of the structure and the latter is mainly the dominant effect of the resonance characteristics of a single scatterer (Hasheminejad & Rajabi, 2007; Kafesaki & Economou, 1995; Lagendijk & Van Tiggelen, 1996). In this paper the vibration characteristics of a phononic crystal structure surface comprising of periodic split cylinders with varying diameters is experimentally and numerically studied to provide some reference value for its practical use.

2. Computing method

In this paper, we consider a cell with multiple split cylinders of different diameters within a square latticemembrane and its vibration characteristics in a cylindrical structure. The cell structure is composed of an aluminum membrane and a glass wool material embedded in cylinders as wave scatterers. The phononic crystal structure is surrounded by vacuum therefore its dispersion relation in an infinite system is considered and calculated. A control equation for the propagation of an elastic wave in a solid structure is applied.

$$\sum_{j=1}^3 \frac{\partial}{\partial x_j} \left(\sum_{l=1}^3 \sum_{k=1}^3 C_{ijkl} \frac{\partial u_k}{\partial x_l} \right) = \rho \frac{\partial^2 u_i}{\partial t^2} \quad (i = 1, 2, 3) \quad (1)$$

where, ρ is the mass density, C_{ijkl} is the elastic constant, u_i is displacement, t is time $x_j (j=1,2,3)$ corresponds to the coordinate variable x,y and z. As the infinite system is arranged periodically in the X and Y direction, it is easier to apply a Bloch-Floquet periodicity to the boundaries of the unit cell structure. Through the application of periodicity on the phononic crystal structure the vibration characteristics can be converted into the unit cell structure by introducing periodic boundary conditions along the X~Y direction. The wave vector parameter K is introduced into the periodic boundary condition within the first irreducible Brillouin boundary of the unit cell structure to solve the eigenvalues of the spectra problem which describes the vibration characteristics of the whole phononic crystal structure. In this paper a multiple split cylinder cell structure made of an aluminum mass membrane plate and glass wool stuffed into cylinders to form a unit cell. The radius of the multiple split cylinders is given as r and lattice constant a , $a = 24mm$, $r = 11.8mm \sim 3.6mm$ with a thickness of $t = 0.6mm$ as presented in **Fig.1**

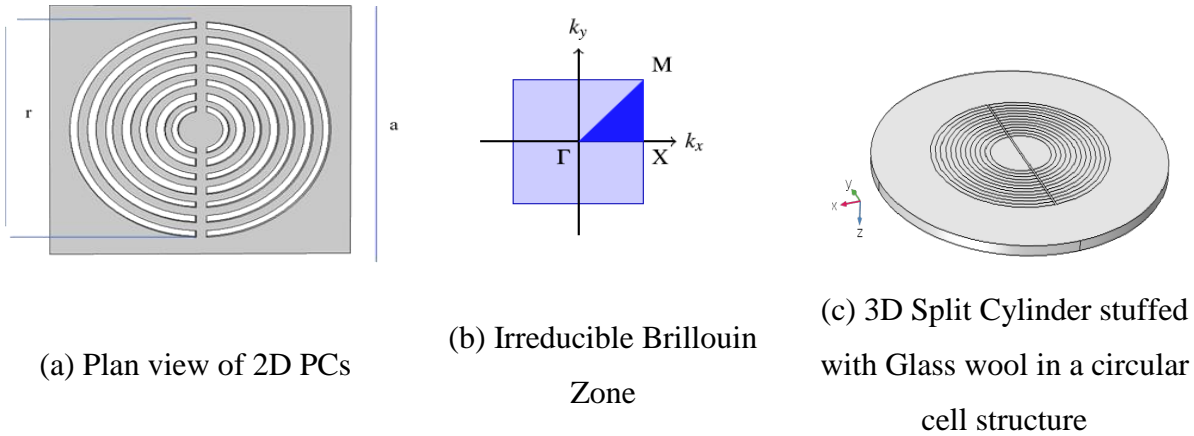


Fig. 1 Unit Cell Structure

Table 1 Material Properties

Material	Density	Poisson ratio	Young Modulus
Aluminum	$2700kg / m^3$	0.32	$70GP_a$
Glass wool	$200kg / m^3$	0.23	$2100P_a$

The bandgap characteristics defines the positions within the PCs structure where the propagation of elastic waves is prohibited. To determine the bandgap characteristics of the structure and the resonant effects of the Phononic split cylinder crystal structure, the finite element method in the commercial software Comsol Multiphysics is used (FEM). The PCs structure show two broad bandwidth, low frequency bandgap characteristics of between 48~70Hz and 83~128Hz. The low frequency bandgap characteristics is presented in **Fig.2**.

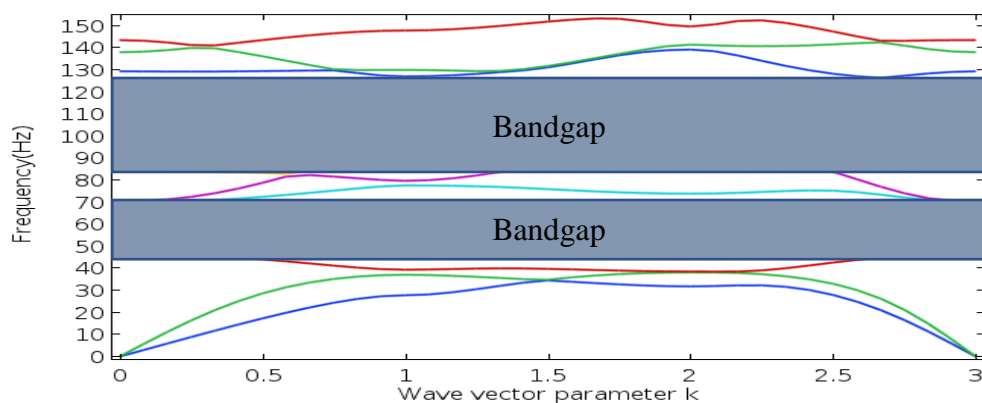


Fig.2 Bandgap characteristics of PCs $a_1 = a_2 = 24mm$, $r_1 = r_{14} = 11.8mm \sim 3.6mm$

3. Experimental Analysis

Due to bandgap characteristics of acoustic metamaterials, the corresponding vibration transfer characteristics are based on the ideal assumption that the transverse and longitudinal directions are infinite cycles. However, in practical engineering applications this assumption is very difficult to achieve. In the experimental setup, to determine the vibration characteristics of the PCs structure, four split cylinder cells were placed in a circular aluminum plate membrane. A sandwich aluminum circular plate with glass wool stuffed into the split cylinders was used. The circular plate has a diameter of $60mm$ with four evenly spaced split cylinders across its surface. The phononic crystal structure model for study is labeled as **model-1**.

To have a standard measure for comparison and analysis of vibration characteristics results of the PCs structure a second model with same number of split cylinders across its surface is designed, however the thickness of the plate and glass wool thickness in the second structure labeled as **model-2** is varied to be higher than the first split cylinder PCs structure in order to investigate the effects of structural thickness on vibrational characteristics on the PCs structure.

The PCs structure **model-1** is made up of an aluminum membrane of thickness $6.5mm$ with a glass wool thickness of $6.5mm$ stuffed into its split cylinders. The second split cylinder PCs structure for experimental comparison is made from a thin plate of thickness $9mm$ and glass wool thickness $10mm$ labeled **model-2**. The experimental setup in terms of component arrangement is presented in Fig.3,



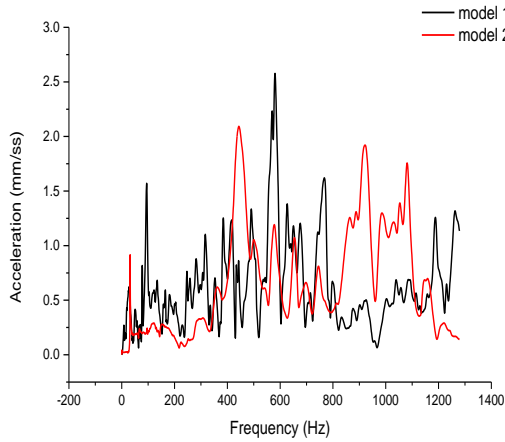
(a) Model-2

(b) Model-1

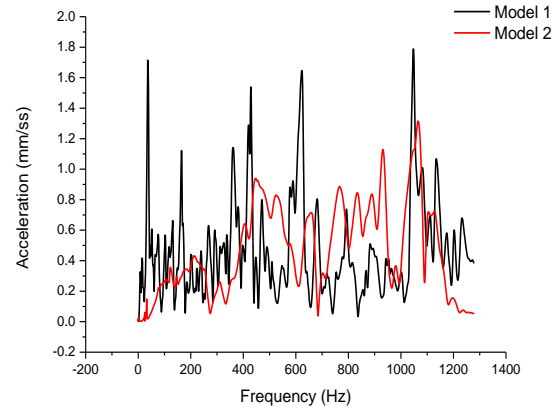
Fig.3 Experimental setup

As shown in Fig.3 the experimental measurement and analysis system includes a computer, signal acquisition system, impulse hammer, impulse acceleration sensor, and an experimental PCs structure model (model-1 and model-2). The experiment was conducted in a frequency range of 0~1400Hz in a single direction along the z-axis. The vibration characteristics were calculated along three excitation points across the surface of the PCs models 1~2. The impulse hammer serves as a testing point for analyzing natural frequencies, modal masses, modal damping ratios and mode shapes of the PCs structure surface. The PCs structure and its vibration characteristics are analyzed through the acceleration of impulse propagating waves across the surface of the split cylinder units. In the experiment, a super soft rubber tip impact point is fixed to the impulse hammer with an upper frequency of 200Hz. The impulse hammer was used to strike the surface of the split cylinder cells individually while the resulting impact propagating waves are measured across the excitation points 1, 2 and 3 of the impulse acceleration sensor. The main idea of arranging the impulse acceleration sensors close to the split cylinder cells within areas of maximum impact displacement was to investigate the effects of the split cylinders in suppressing the vibration displacement characteristics of the impulse propagating waves across the surface of the PCs structure.

3.1 Results and Discussion



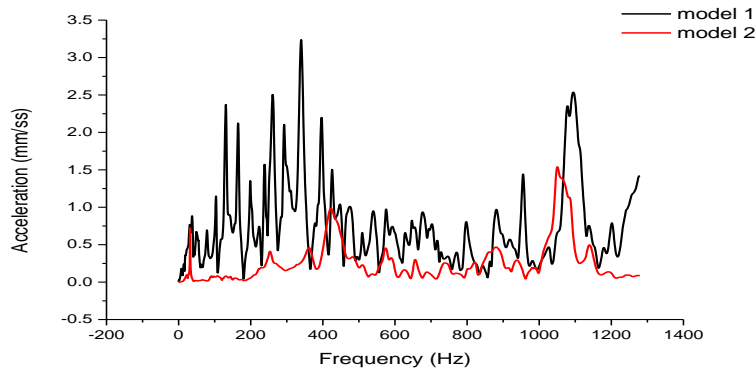
(a) Point 1



(b) Point 2

Fig.4 Vibration Characteristics along point 1~2.

The vibration characteristics are observed when the impulse hammer is used to strike the surface of the PCs structures model-1 and model-2. The impulse acceleration sensor captures the vibrational characteristics of the impact of the hammer across the surface of the models at excitation points 1~3 along the z-direction. The vibration characteristics along the first and second excitations points captured by the acceleration sensor is presented in Fig.4. Results show Model-1 having a high vibration characteristics displacement peaks at excitation points 1 and 2 within the low frequency range. Model-2 however has low vibration displacement characteristic peak in the high frequency range. Relative decrease and increase in displacement amplitude vibration characteristics in the high frequency range shows low to high damping characteristics in the PCs structures.



(b) Point 3

Fig.5 Vibration Characteristics along point 3

Model-1 show high vibration displacement characteristics along excitation point~3 in the low frequency range compared to the characteristics of **model-2** which has good displacement characteristics in the high frequency. Both PCs structures have good vibration displacement characteristics, however Model-1 is more effective based on the fact that it has good vibration displacement characteristics in the low frequency range.

3.2 Numerical Simulation

In the finite element calculation, the frequency response function of the structure with infinite period in the y-direction is calculated. In vibration theory, acoustic transmission characteristics is described using frequency response function between structural excitation and response end. If the physical quantity is taken as the excitation end and the response end, the frequency response function is a dimensionless scale factor called the transmission rate or loss usually expressed as twenty times their logarithm.

$$TL = 20 \log \left[\frac{x_1}{x_2} \right] \quad (2)$$

Where x_1 and x_2 represent the excitation and response ends respectively. Using finite element method, a periodic boundary condition is applied to the upper and lower boundaries of the 6th-cycle along the x, y directions. The length of the plate structure is set to a PML boundary at both ends of the cell structure. The calculation is done within a frequency of 100~2000Hz. The transmission is calculated using equation 2, results of the of the transmission is presented in Fig.6,

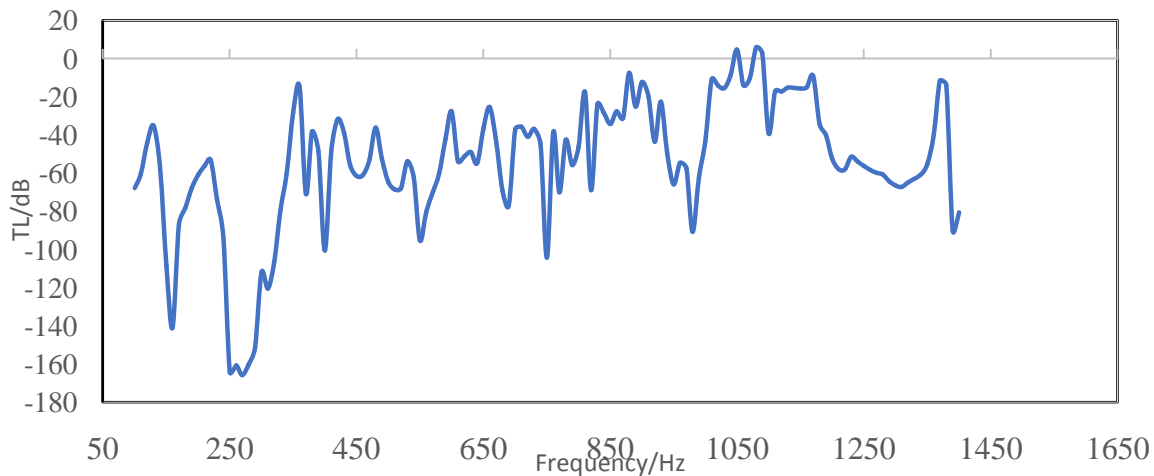


Fig.6 Transmission loss using six cell structures under perfectly matched boundary layer condition.

Analyzing the results of the transmission loss from Fig.6, the attenuation function of the frequency response function in the low frequency range of 50~270Hz is very large, resulting in the occurrence of a vibration bandgap which is just a little above the unit cell structure bandgap of 48~70Hz and 83~128Hz.

4. Conclusion

In this paper, the vibration characteristics of a split cylinder structure has been studied. The bandgap characteristics, vibration displacement characteristics and vibration transmission rate have all being predicted, in summary the following observations have been made,

- through finite element methods the split cylinder structure can obtain wide vibration bandgap characteristics in the low frequency range of 48~70Hz and 83~128Hz.
- through one-dimensional vibration experiment in the z-direction, the split cylinder structure surface can displace low frequency vibration characteristics.
- through finite element methods calculations six split cylinder structures under perfectly matched boundary conditions shown a low vibration transmission loss of -165dB at a low frequency range of 270Hz.
- thickness of plate and glass wool inclusions have effects on the damping of the structure in the low and high frequency range.
- material parameter variations have an impact on the vibration characteristics across the surface of the split cylinder structure.

References

- Aki, K., & Larner, K. L. (1970). Surface motion of a layered medium having an irregular interface due to incident plane SH waves. *Journal of geophysical research*, 75(5), 933-954.
- Baravelli, E., & Ruzzene, M. (2013). Internally resonating lattices for bandgap generation and low-frequency vibration control. *Journal of Sound and Vibration*, 332(25), 6562-6579.
- Cheng, Y., Liu, X., & Wu, D. (2011). Band structure of a phononic crystal plate in the form of a staggered-layer structure. *Journal of Applied Physics*, 109(6), 064904.
- Del Vescovo, D., & Giorgio, I. (2014). Dynamic problems for metamaterials: review of existing models and ideas for further research. *International Journal of Engineering Science*, 80, 153-172.
- Goffaux, C., & Sánchez-Dehesa, J. (2003). Two-dimensional phononic crystals studied using a variational method: Application to lattices of locally resonant materials. *Physical Review B*, 67(14), 144301.
- Hasheminejad, S. M., & Rajabi, M. (2007). Acoustic resonance scattering from a submerged functionally graded cylindrical shell. *Journal of Sound and Vibration*, 302(1-2), 208-228.
- Hsu, J.-C. (2011). Local resonances-induced low-frequency band gaps in two-dimensional phononic crystal slabs with periodic stepped resonators. *Journal of Physics D: Applied Physics*, 44(5), 055401.
- Jensen, J. S. (2003). Phononic band gaps and vibrations in one- and two-dimensional mass-spring structures. *Journal of Sound and Vibration*, 266(5), 1053-1078.

- Kafesaki, M., & Economou, E. (1995). Interpretation of the band-structure results for elastic and acoustic waves by analogy with the LCAO approach. *Physical Review B*, 52(18), 13317.
- Kushwaha, M. S. (1996). Classical band structure of periodic elastic composites. *International Journal of Modern Physics B*, 10(09), 977-1094.
- Kushwaha, M. S., Halevi, P., Dobrzynski, L., & Djafari-Rouhani, B. (1993). Acoustic band structure of periodic elastic composites. *Physical review letters*, 71(13), 2022.
- Lagendijk, A., & Van Tiggelen, B. A. (1996). Resonant multiple scattering of light. *Physics Reports*, 270(3), 143-215.
- Laude, V. (2015). *Phononic Crystals: Artificial Crystals for Sonic, Acoustic, and Elastic Waves* (Vol. 26): Walter de Gruyter GmbH & Co KG.
- Liu, L., & Hussein, M. I. (2012). Wave motion in periodic flexural beams and characterization of the transition between Bragg scattering and local resonance. *Journal of Applied Mechanics*, 79(1), 011003.
- Liu, Z., Chan, C. T., & Sheng, P. (2002). Three-component elastic wave band-gap material. *Physical Review B*, 65(16), 165116.
- Lu, M.-H., Feng, L., & Chen, Y.-F. (2009). Phononic crystals and acoustic metamaterials. *Materials today*, 12(12), 34-42.
- Maldovan, M. (2013). Sound and heat revolutions in phononics. *Nature*, 503(7475), 209.
- Ramakrishna, S. A. (2005). Physics of negative refractive index materials. *Reports on progress in physics*, 68(2), 449.
- Shen, L., Wu, J. H., Liu, Z., & Fu, G. (2015). Extremely low-frequency Lamb wave band gaps in a sandwich phononic crystal thin plate. *International Journal of Modern Physics B*, 29(05), 1550027.
- Sridhar, A., Kouznetsova, V. G., & Geers, M. G. (2016). Homogenization of locally resonant acoustic metamaterials towards an emergent enriched continuum. *Computational mechanics*, 57(3), 423-435.
- Su, Z., Ye, L., & Lu, Y. (2006). Guided Lamb waves for identification of damage in composite structures: A review. *Journal of Sound and Vibration*, 295(3-5), 753-780.
- Sun, J., Jolly, M. R., & Norris, M. (1995). Passive, adaptive and active tuned vibration absorbers—a survey. *Journal of mechanical design*, 117(B), 234-242.
- Wagner, M. R., Graczykowski, B., Reparaz, J. S., El Sachat, A., Sledzinska, M., Alzina, F., & Sotomayor Torres, C. M. (2016). Two-dimensional phononic crystals: Disorder matters. *Nano letters*, 16(9), 5661-5668.
- Xiao, W., Zeng, G., & Cheng, Y. (2008). Flexural vibration band gaps in a thin plate containing a periodic array of hemmed discs. *Applied Acoustics*, 69(3), 255-261.
- Xiao, Y., Wen, J., & Wen, X. (2012). Flexural wave band gaps in locally resonant thin plates with periodically attached spring–mass resonators. *Journal of Physics D: Applied Physics*, 45(19), 195401.